



SEISMIC RETROFIT OF NON-DUCTILE RECTANGULAR REINFORCED CONCRETE COLUMNS BY CFRP JACKETING

Alper ILKI¹ Aynur TEZCAN² Volkan KOC³ Nahit KUMBASAR⁴

SUMMARY

In this paper, experimental results on the behavior of non-ductile rectangular columns retrofitted by carbon fiber reinforced polymer (CFRP) jackets are presented. 8 specimens constructed with low strength concrete, plain bars and without adequate transverse reinforcement were tested under constant axial and reversed cyclic lateral loads. The lap splice lengths of longitudinal reinforcement for four of the specimens were inadequate, while the longitudinal bars were continuous for the remaining four specimens. In each of these two groups; one specimen was tested as the reference specimen, 2 specimens were retrofitted with different thicknesses of transverse CFRP jackets, and one previously damaged specimen was retrofitted with CFRP jacket after repairing procedure. Test results indicated that significant ductility enhancement can be obtained for low strength brittle concrete columns retrofitted by CFRP jackets. For the specimens with inadequate lap splices, the enhancement in ductility was not as remarkable as the specimens with continuous longitudinal reinforcement.

INTRODUCTION

Structural members are expected to perform a ductile behavior during earthquakes. The structural members may experience damage due to inelastic response but they should survive after earthquakes. Confinement of structural members is a well known and very effective way to obtain ductile behavior, [1-5]. Many researchers showed that under axial loading significant enhancement in terms of strength and ductility can be obtained by confining concrete members with FRP materials, [6-14]. Confinement of columns also helps preventing buckling of longitudinal rebars and retarding loss of bond due to inadequate lap splice length. Besides being relatively expensive than the conventional techniques like concrete or steel jacketing, usage of FRP jacketing system has many important advantages like easy and quick application, low weight to strength ratio and high durability. An additional advantage of retrofitting with FRPs is that the weight of the structure and the dimensions of the members do not increase.

¹ Assist. Prof. Dr., Faculty. of Civ. Eng., Istanbul Tech. Univ., Istanbul , Turkey, ailki@ins.itu.edu.tr

² Post Grad. St., Faculty. of Civ. Eng., Istanbul Tech. Univ., Istanbul, Turkey, aynurtezcan@hotmail.com

³ Post Grad. St., Faculty. of Civ. Eng., Istanbul Tech. Univ., Istanbul, Turkey, kocv@myinet.com

⁴ Prof. Dr., Faculty. of Civ. Eng., Istanbul Tech. Univ., Istanbul , Turkey, kumbasar@ins.itu.edu.tr

Since most of the existing structures in Turkey and other developing countries were not constructed according to the current design codes, they have some vital deficiencies like low concrete quality, inadequate transverse reinforcement, inadequate lap splice lengths and poor reinforcement detailing. Because of these and other potential deficiencies, many of the existing structures need to be rehabilitated to enhance the overall structural performance. Various experimental studies have been carried out to investigate the behavior of columns retrofitted by CFRP sheets under combined axial and lateral loads, [15-21].

In this study, the behavior of non-ductile columns retrofitted by CFRP jackets is examined. Experimental work, conducted at Istanbul Technical University (ITU) Structural and Earthquake Engineering Laboratory, consisted of 8 specimens with rectangular cross section of 200mm×300mm which were tested under constant axial and reversed cyclic lateral loads. All these 8 specimens were constructed with inadequate transverse reinforcement and low quality concrete like many existing structures in Turkey (concrete strength of the members, f_{coj} , at the day of testing day were around 10 MPa). Plain bars were used for both longitudinal and transverse reinforcement for representing most of the existing structures which were built around 1970s and 1980s. Longitudinal reinforcing bars of the 4 of the specimens were continuous, while the other 4 specimens had lap-splices of 40×diameter of longitudinal bars, whereas the lap-splice lengths should have been around 80×diameter of longitudinal bars considering the yield strength and the type of the reinforcing bars and the concrete quality. In each main group, one specimen was tested as a reference specimen while the others were tested after being retrofitted by different thicknesses of transverse CFRP jackets. All of the specimens were reinforced such that shear failure would be avoided. The spacing of transverse reinforcement in the confining zones of columns was 200 mm while in the other regions it was 100 mm. With this detail it was guaranteed that the damage would occur in the confining zones. Reinforcement details can be seen in Fig. 1.

SPECIMEN DETAILS

Specimens which had rectangular cross section (200 mm width, 300 mm depth and 3000 mm length) were reinforced specially to ensure damage to occur in the confining zones. Plain bars with 14 and 8 mm diameter were used for longitudinal and transverse reinforcement, respectively. Reinforcement details are given in Table 1. Longitudinal reinforcement ratio (ρ_l) was 0.01 and the volumetric transverse reinforcement ratio (ρ_h) at the confining zones was 0.0037 for all specimens.

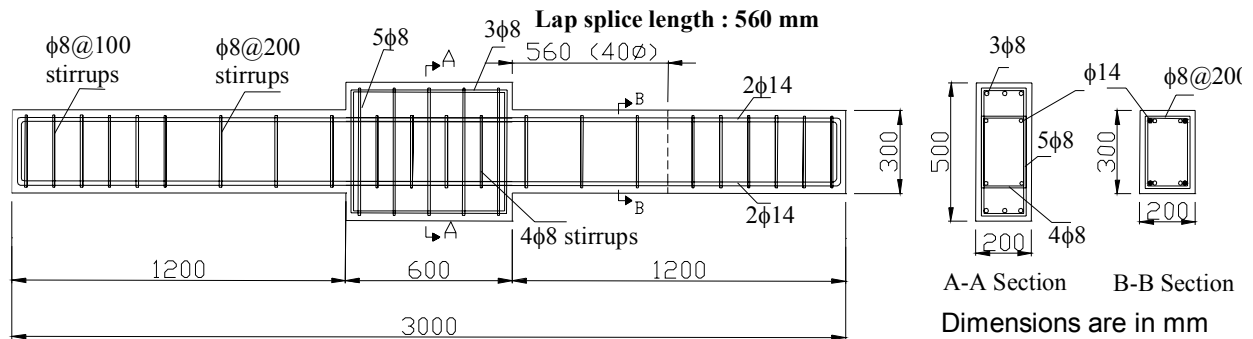


Fig. 1. Details of the test specimens

In Table 1, f_y , f_{su} and f_s represent the yielding stress, ultimate stress and tensile stress of the reinforcement, respectively. ϵ_y and ϵ_{su} are tensile strains corresponding to f_y and f_{su} , respectively.

Table 1. Reinforcement details

Reinforcement	Diameter (mm)	f_y (MPa)	ϵ_y	f_{su} (MPa)	ϵ_{su}	f_s (MPa)	Modulus of Elasticity (MPa)
Longitudinal	14	336	0.002	344	0.290	487	216000
Transverse	8	383	0.002	392	0.284	564	203000

For construction of specimens, specially designed ready mixed concrete with water/cement ratio of 1.06 was used. Ordinary Portland cement (Set Marmara Cement) class 42.5 and fly ash from Catalagzi, Cayirhan were used in the mixture. Powdered stone and coarse aggregate were from Cebeci Dalbay with the maximum size of 0.7 and 15 mm, respectively. Sand was from Akpınar Sulun Mine with maximum size of 0.5 mm. Mid-range water reducer Grace WRDA 90W was used as superplasticizer in the mixture. Mix proportion is presented in Table 2. The average compressive strengths were 9.22 MPa at 28 days, 12.96 MPa at 90 days, and 13.41 MPa at 150 days.

Table 2. Concrete mix proportions (kg/m³)

Cement	Water	Sand	Powdered Stone	Coarse Aggregate	Superplasticizer	Fly-ash
155	165	670	303	987	1.22	40

According to the Turkish Standards TS500-2000 [22], lap splice length can be determined by using the design yield strength of the reinforcing bar (f_{yd}) and the design tensile strength of the concrete (f_{ctd}). Lap splice length, l_o , is directly related with the anchorage length, l_b , and can be calculated by the Eq. (1),

$$l_o = c \times l_b \quad (1)$$

where $c=1.5$ if all lap splices are formed at the same section. The anchorage length for plain reinforcement can be calculated by Eq. (2),

$$l_b = 0.24 \times d \times (f_{yd}/f_{ctd}) \quad (2)$$

where d is the diameter of the bar. According to these equations lap splice length should have been about $80 \times d$ (1120 mm) with the common design values of the materials of 1960s and 1970s (concrete characteristic compressive strength $f'_c=14$ MPa, steel characteristic yield strength $f_y=220$ MPa). However, lap splice length was $40 \times d$ (560 mm) for four specimens, which were designed for examining the behavior of rc members with inadequate lap splice length. Note that as the actual yield strength of longitudinal bars was higher and concrete compressive strength was lower than the values used for design, so for actual strength values the necessary lap splice length was about $145 \times d$.

The selected prototype columns and joints were designed considering lower stories of a typical non-ductile moment-resisting frame of 1960s, 1970s. Generally, during design phase for the columns of lower stories of typical 4~5 story structures in Turkey, the level of dimensionless axial load (v) is around 30%. However, since the actual concrete quality is lower than assumed during design phase, the dimensionless axial load level may increase significantly. 252 kN constant axial load was applied to the specimens during experiments and axial load ratio (v) was obtained by Eq. (3),

$$v = N / f'_{coj} A_g \quad (3)$$

where N is the applied axial load, A_g is the gross cross sectional area and f'_{coj} is the compressive strength of the concrete in the member at the specified ages. Note that f'_{coj} corresponds to 85% of the standard cylinder strength at the specified ages.

Concrete quality, reinforcement details and lap splice length (if specimen was lapped spliced) were all same for all specimens. Axial force ratio (ν), was between 0.37 and 0.47. The general properties of the specimens are presented in Table 3.

Table 3. General properties of the specimens

Specimen	General explanation	Retrofit detail	Age (days)	f'_{cj} (MPa)	f'_{coj} (MPa)	ν
C-O-1	Original-continuous reinforcement	-	51	10.61	9.02	0.47
LS-O-1	Original-lap spliced	-	58	11.03	9.38	0.45
R-C-C-3	Retrofitted-continuous reinforcement	3 plies of CFRP	164	13.41*	11.40	0.37
R-LS-C-3	Retrofitted-lap spliced	3 plies of CFRP	170	13.41*	11.40	0.37
R-C-C-6	Retrofitted-continuous reinforcement	6 plies of CFRP	192	13.41*	11.40	0.37
R-LS-C-6	Retrofitted-lap spliced	6 plies of CFRP	181	13.41*	11.40	0.37
R-R-C-C-6	C-O-1, after repair and retrofit	6 plies of CFRP	216	13.41*	11.40	0.37
R-R-LS-C-6	LS-O-1, after repair and retrofit	6 plies of CFRP	232	13.41*	11.40	0.37

* : Because there is no standard cylinder compression tests after 150 days, the strength of the specimens older than 150 days were assumed same as the strength of the 150 days old specimens.

For retrofitting, confining zones were wrapped by CFRP sheets. The purpose of retrofitting was to obtain ductile behavior by providing confinement, prevent buckling of longitudinal bars, which might cause premature failure and to retard slip of reinforcement for the specimens with inadequate lap splices by limiting lateral deformations.

For repair of pre-damaged specimens, damaged zones were filled with repair mortar with compressive strength of 50 MPa after removing all loose and damaged concrete. For retrofitting, confining zones were jacketed externally by unidirectional CFRP sheets in transverse direction with 0-degree orientation after 7 days from repairing. Before wrapping the confining zones with CFRP sheets, surface preparation procedure was carried out, which included sanding, cleaning, forming one layer of epoxy-polyamine primer and one layer of epoxy adhesive putty. Then epoxy adhesive was used for bonding CFRP sheets on the confining zones. Other layers of epoxy adhesive were applied between the CFRP sheet plies and on the outer ply of CFRP sheet. The compressive and tensile strengths of the epoxy system were around 80 and 50 MPa, respectively. Tensile elasticity modulus of the epoxy system was around 3000 MPa and its ultimate elongation was 0.025. The steps during wrapping need to be carried out with great care to prevent stress concentrations due to surface irregularities and to obtain the tight fitting of the CFRP sheets on the specimens. CFRP sheets were wrapped continuously, and for obtaining satisfactory bonding, 200 mm overlap length was made at the end of the wrap. The geometrical and mechanical properties of the CFRP sheets are given in Table 4. FRP materials behave linear elastic till rupture. The effective thickness of the used CFRP sheets was 0.165 mm for one layer.

Table 4. Geometrical and mechanical properties of CFRP

Characteristic tensile elasticity modulus (MPa)	230000
Maximum elongation (%)	1.5
Characteristic tensile strength (MPa)	3430
Tensile strength with 200 mm overlap (MPa)	3430
Unit weight (kg/m^3)	1820
Effective area per unit width (mm^2/mm)	0.165

TEST SETUP

The column units were subjected to simulated seismic loads at the Structural and Earthquake Engineering Laboratory of Istanbul Technical University. All specimens were tested under combined axial load and reversed cyclic lateral loads. Specimens were tested in horizontal position, Fig. 2. Reversed cyclic lateral loads were applied vertically to the stub at the mid-height of the specimens. A 250 kN capacity MTS servo-controlled hydraulic actuator was used to apply the lateral load and to perform the displacement controlled hysteresis loops.

A single curvature bending was obtained over the whole height of specimens. This differs from the actual case in a moment-resisting frame, the input moments of the beams causes the sign of the curvature to be different above and below the beam-column joint. In tests investigating the beam-column joint cores, a method of loading that causes a change in the sign of the column curvature above and below the joint is necessary, because of the significant shear and bond stresses induced by the sign of the curvature. However, in tests investigating the behavior of the plastic hinge regions at the ends of the columns, the simulation of the exact stress conditions in the beam-column joint core is not so important, Rodriguez [19], Park [23], Priestley [24].

Constant axial load was maintained by post-tensioning four $\frac{3}{4}$ inch (19.05 mm) diameter high strength prestressing tendons with a hydraulic jack at one end of the specimens. A manually controlled 600 kN Enerpac hydraulic jack was used for this purpose.

Instrumentation system consists of linear variable displacement transducers (LVDT), internal and external load cells, and electrical resistance strain gages. Measurements from these instruments were acquired by a TML TDS-303 data logger via a TML ASW-50-C switch box. Lateral displacements and the rotation of central stub were measured with a pair of TML SDP-200D displacement transducers. All tests were conducted under displacement control, and control displacement was obtained by averaging these two transducers. At both sides of the stub, 12 TML CDP-50 displacement transducers with 50 mm stroke length were used to measure the average section curvatures. Bolts holding the curvature transducers were embedded into the core concrete, and stroke tips of these transducers were in contact with the stub faces. Curvatures of the potential hinging zones were measured over 150 and 300 mm gage lengths. Several other displacement transducers were also used to monitor reliability and safety of the experiments. Lateral flexural load acted by the MTS hydraulic actuator was measured with a 250 kN internal load cell, and the applied axial load was measured by a 1000kN TML CLP-100CMP load cell. Test setup and the positions of all displacement transducers are presented in Fig. 2.

In order to measure the longitudinal and transverse reinforcement strains in the potential plastic hinging region, several strain gages were bonded on these bars, Fig. 3. While most of them were TML YFLA-5 post-yield strain type, a few were TML FLA-5 type ordinary foil gage. At peak displacement levels, the observed damage was recorded with photographs, videos, and sketches.

Loading Pattern

At each test, a sequence of reversed cyclic flexural loads was applied combined with a constant axial load. Applied axial load was 252 kN for all specimens. This corresponds to a range of axial load ratios between 0.37 and 0.47 obtained by Eq. (3). This axial load ratio range is quite realistic especially for lower stories of existing structures with moment-resisting frames constructed with low strength concrete. After applying the axial load, the lateral displacements were imposed until the selected target levels. As shown in Fig. 4, the cyclic loading history can be divided into two phases. First phase, namely the elastic phase, included target displacements corresponding to the drift ratios of ± 0.0020 (± 2.8 mm), ± 0.0025 (± 3.5 mm), ± 0.0035 (± 4.9 mm), and ± 0.0050 (± 7.0 mm). In the inelastic second phase, target displacements were determined according to the reference yield displacement, δ_y . The δ_y displacement was defined as the displacement of the C-O-1 reference column at the stub when the tensile reinforcement first yielded, (9.5 mm). The columns

were subjected to two pulling and pushing cycles at displacement ductility ratios of $\mu = \pm 1.0, \pm 1.5, \pm 2.0, \pm 2.5, \pm 3.0, \pm 3.5, \pm 4, \pm 4.5, \pm 5, \pm 5.5, \text{ and } \pm 6$, where μ is the displacement ductility factor defined as δ/δ_y . δ was the average lateral displacement of the central stub. Ductility displacement ratio, $\mu = \pm 6.0$ could only be applied in the case of continuously reinforced specimens.

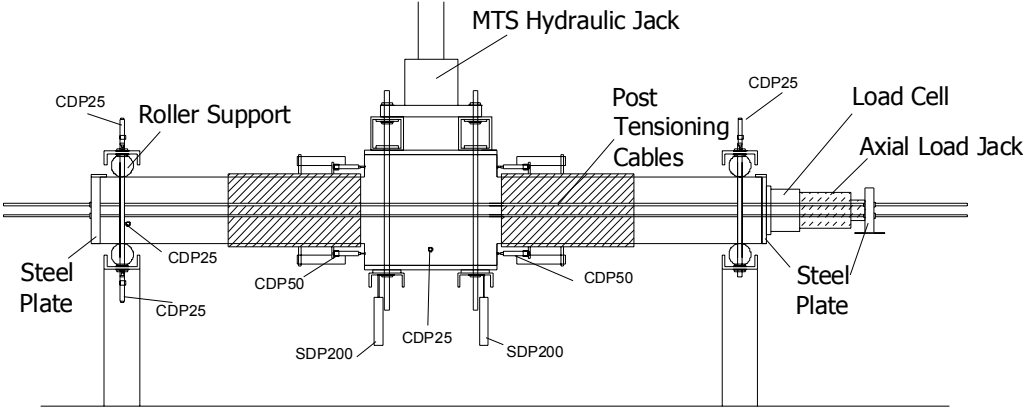


Fig. 2. Test setup and instrumentation

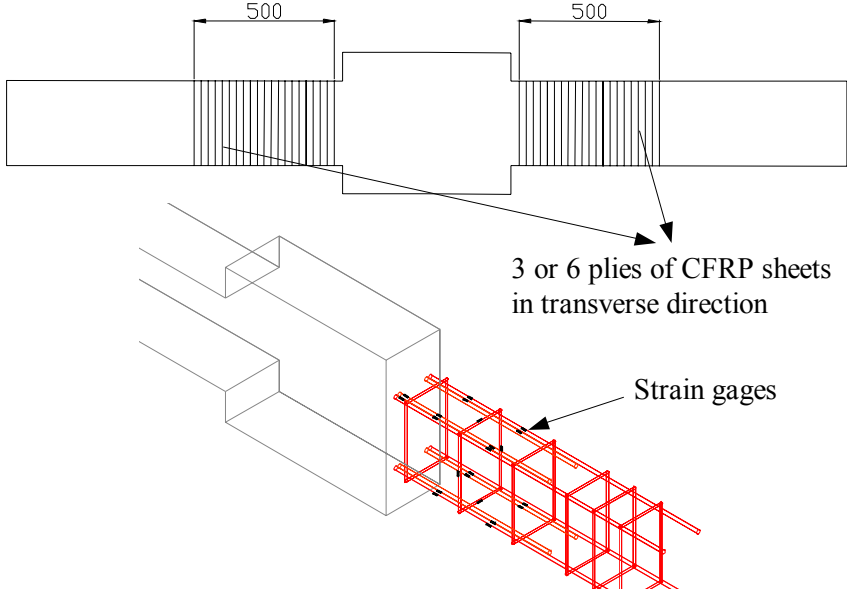


Fig. 3. Retrofitting regions and locations of the strain gauges

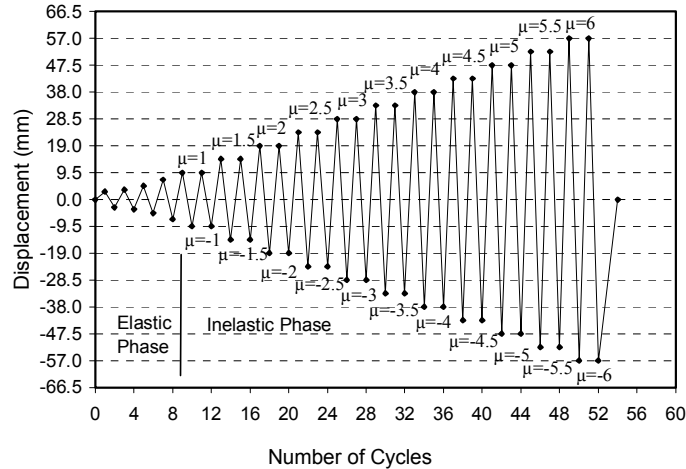


Fig. 4. Loading pattern

TEST RESULTS

Specimen C-O-1

This is the reference specimen with continuous longitudinal bars. The lateral load versus lateral displacement hysteresis loops measured at the stub is shown in Fig. 5. All load-displacement relationships were obtained considering the load acted by the MTS hydraulic actuator and the average displacement measured under the stub. First flexural cracks were observed at the displacement of 2.8 mm (0.002 drift ratio). In the following elastic cycles, cracks were scattered on both upper and lower columns through the first 300 mm zones from the stub faces. After the displacement ductility level of $\mu = 1.0$ (9.5 mm) cracks were concentrated and widened in the first 150 mm zone of both columns. At the displacement ductility level of $\mu = \pm 1.5$ (± 14.25 mm) concrete crushing was observed at the load level of 71 kN. In the following cycles cracks concentrated on the lower column and at the first cycle of displacement ductility level $\mu = -2.0$ (-19 mm), lower column concrete cover was spalled off. At the second cycle of displacement ductility level $\mu = -2.0$ (-19 mm), significant strength degradation was observed due to buckling of the longitudinal bars in the lower column. While loading was going on for the next target displacement ductility level of $\mu = 2.5$ (+23.75 mm), longitudinal bars of the upper column buckled at the displacement level of +14 mm and test was stopped due to very high level of strength degradation. Damage pattern for specimen C-O-1 is given in Fig. 5.

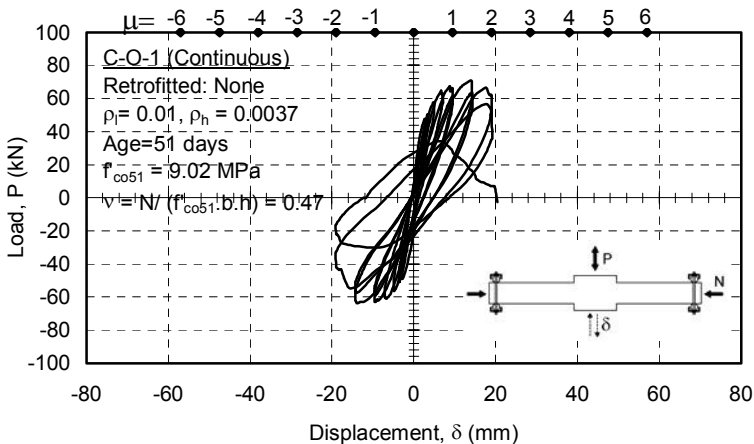


Fig 5. Load-Displacement relationship and the appearance of the specimen C-O-1

Specimen R-C-C-3

Specimen R-C-C-3 was retrofitted by 3 plies of CFRP sheets. The lateral load versus lateral displacement relationship measured at the stub is shown in Fig. 6. First bending crack was observed around the stub faces at $\delta=2.0$ mm ($F=45$ kN) in pushing and at $\delta =-2.1$ mm ($F=-59$ kN) in pulling cycles. Maximum lateral load of 84 kN was reached at the first displacement ductility of $\mu=+1.5$ (+14.25 mm) while concrete crushing began. Concrete crushing got clear and crack widths were between 4-8 mm when displacement ductility was $\mu=+3.5$ (+33.25 mm). In the displacement ductility levels of $\mu=\pm 4.5$ (± 42.75 mm), lateral load capacity was between ± 65 - ± 70 kN and significant damage could be observed on the specimen and concrete cover were spalled off around supports due to reinforcement slip. Lateral load capacity decreased and damage increased gradually in the following displacement levels. Test was stopped after completing the displacement ductility levels $\mu=\pm 6.0$ (± 57 mm) when the load carrying capacity was 50 kN for pushing and -46 kN for pulling. Observations on the damaged specimen, showed that longitudinal reinforcement and hooks at the supports slipped and slippage caused slight damage around supports. R-C-C-3 specimen at the end of the test is shown in Fig. 6.

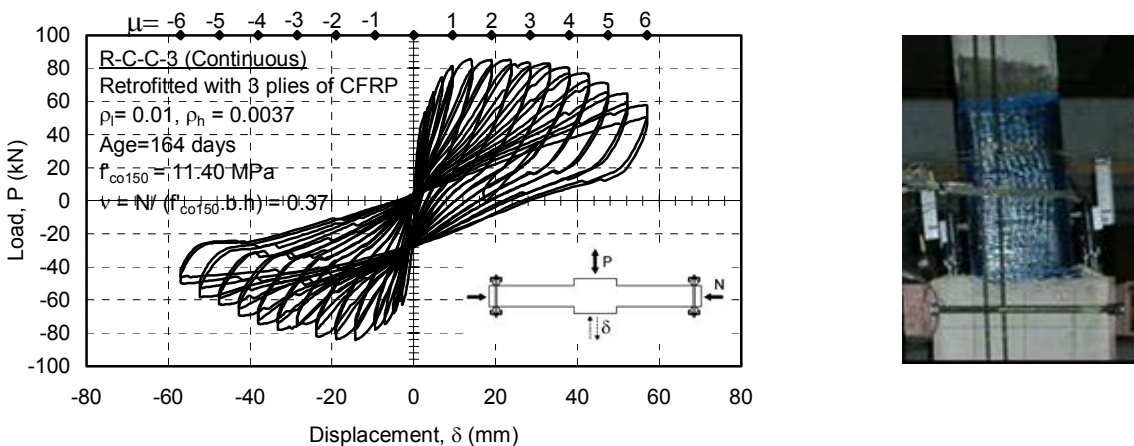


Fig. 6. Load-Displacement relationship and the appearance of the specimen R-C-C-3

Specimen R-C-C-6

Specimen R-C-C-6 retrofitted by 6 plies of CFRP sheets. The lateral load versus lateral displacement relationship measured at the stub is shown in Fig. 7. First bending crack was observed around the stub faces at $\delta=1.9$ mm ($F=45$ kN) in pushing and at $\delta =-2.6$ mm ($F=-56$ kN) in pulling cycles. Cracks were concentrated around the beam column connection and crack widths were changing between 0.8-1.3 mm at the displacement ductility of $\mu= \pm 1.0$ (± 9.5 mm). Maximum load of -83 kN was reached at the first displacement ductility of $\mu=-2.0$ (-19.0 mm). Slight concrete crushing began on the upper column at the second displacement ductility of $\mu=-2.0$ (-19.0 mm). Some damage (cracks at the upper support and concrete spalling at the lower support) around the supports was observed at the second cycle of displacement ductility of $\mu= -3.0$ (-28.5 mm). Damage increased in the following displacement levels while capacity of the specimen was decreased gradually. Lateral load, that specimen was resisting was +60 kN, at the displacement ductility of $\mu=5.5$ (+52.25 mm). Damage in lower and upper columns was almost same in pulling cycles while it was concentrated on the lower column in pushing cycles. Only for this specimen, an additional loading cycle was attempted at the displacement ductility of $\mu=\pm 8.0$ (± 76.0 mm). In these cycles lateral load capacity did not change significantly, however crack widths increased. Specimen R-C-C-6 at the end of the test is shown in Fig. 7.

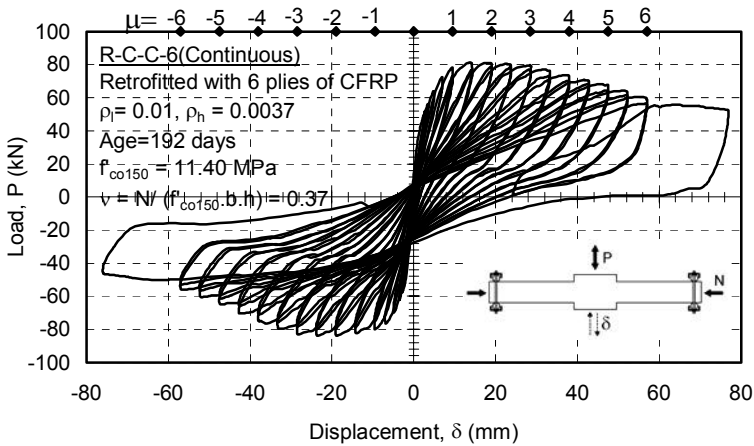


Fig. 7. Load-Displacement relationship and the appearance of the specimen R-C-C-6

Specimen R-R-C-C-6

Specimen R-R-C-C-6 was repaired and then retrofitted by 6 plies of CFRP sheets. The lateral load versus lateral displacement relationship measured at the stub is shown in Fig. 8. The first bending crack was observed around the stub faces at $\delta=2.3$ mm ($F=44$ kN) in pushing and at $\delta=-2.7$ mm ($F=-56$ kN) in pulling cycles. At the first displacement ductility of $\mu=\pm 1.0$ (± 9.5 mm) cycles, lateral load was +79 kN and -92 kN for pushing and pulling cycles, respectively. Maximum load of +91 kN at pushing cycle and -97 kN at pulling cycle was reached at the first displacement ductility of $\mu=\pm 2.0$ (± 19.0 mm) levels. Concrete crushing was observed at the first displacement ductility of $\mu=-3.0$ (-28.5 mm). Out of plane movement was observed at the first displacement ductility of $\mu=-4.0$ (-38.0 mm). Longitudinal bars were buckled at the first displacement ductility of $\mu=-5.5$ (-52.25 mm) level at the beam column connection zone. Test was stopped after completing the displacement ductility of $\mu=\pm 6.0$ (± 57.0 mm) levels due to significant out of plane movement. R-R-C-C-6 specimen at the end of the test is shown in Fig. 8.

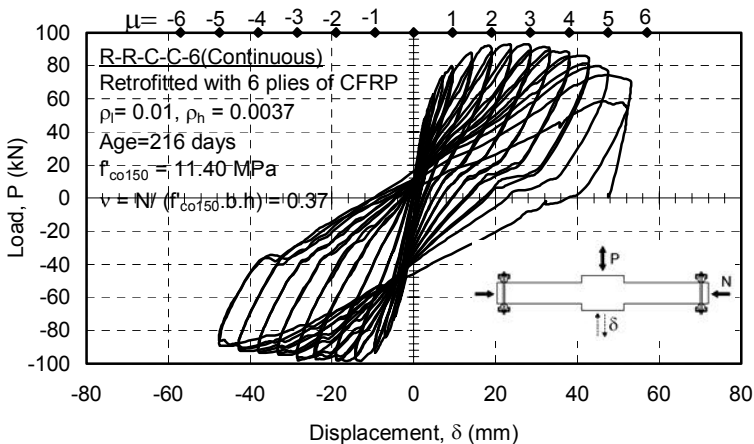


Figure 8. Load-Displacement relationship and the appearance of the specimen R-R-C-C-6

Specimen LS-O-1

This is the reference specimen with lap spliced longitudinal bars in the upper column. The lateral load versus lateral displacement relationship is given in Fig. 9. After the displacement level of +7.0 mm, cracks were concentrated on the upper column where lap splice was located. At displacement level +9.5 mm, 54 kN maximum load was observed. At the second cycle of displacement ductility level $\mu = \pm 1.0$ (± 9.5 mm), longitudinal cracks at the end of the lap splices were observed due to reinforcement slip, Fig. 9. At the displacement ductility level of $\mu = \pm 1.5$ (± 14.25) concrete crushing was observed. During the cycles of ductility levels of $\mu = \pm 2.0$ (± 19 mm) concrete cover spalled off. Test was stopped at the second cycle of displacement ductility level of $\mu = -2.0$ (-19 mm) due to excessive strength degradation. Damage pattern is given in Fig. 9.

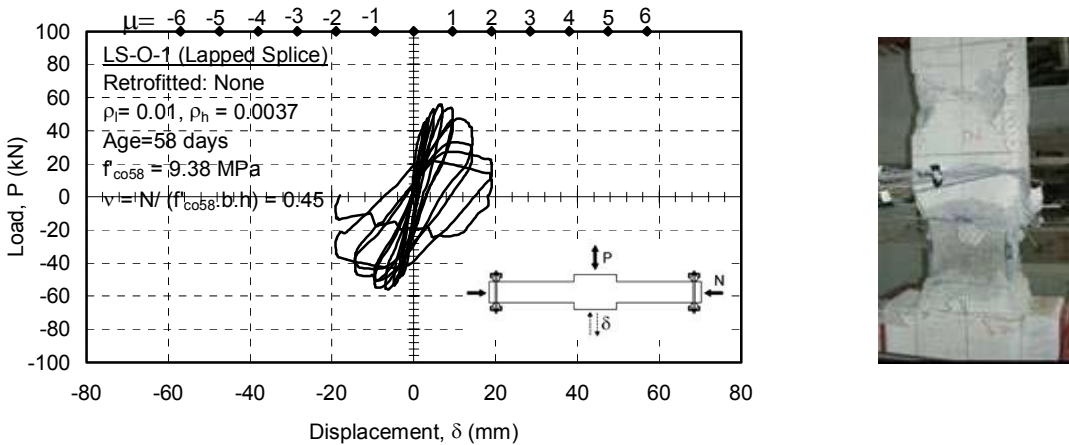


Fig. 9. Load-Displacement relationship and the appearance of the specimen LS-O-1

Specimen R-LS-C-3

Specimen R-LS-C-3 was retrofitted by 3 plies of CFRP sheets. The lateral load versus lateral displacement relationship measured at the stub is shown in Fig. 10. First bending crack was observed around the stub faces at $\delta = 2.0$ mm, ($F = 40$ kN). Concrete began to crush in the compression zones of upper column at the displacement levels of ± 7.0 mm and maximum lateral load was reached, -62 kN, at this level. Damage was almost same on lower and upper column in the elastic cycles. At the displacement ductility of $\mu = +1.0$ (+9.5 mm), cracks were concentrated and widened on the upper story column significantly. Load carrying capacity decreased gradually in the following cycles. The crack widths were between 13-17 mm and 18-21 mm at displacement ductility of $\mu = \pm 4.0$ (± 38.0 mm) and $\mu = \pm 5.0$ (± 47.5 mm), respectively. Test was stopped after completing the cycles of displacement ductility of $\mu = \pm 5.5$ (± 52.25 mm). R-LS-C-3 specimen at the end of the test is shown in Fig. 10.

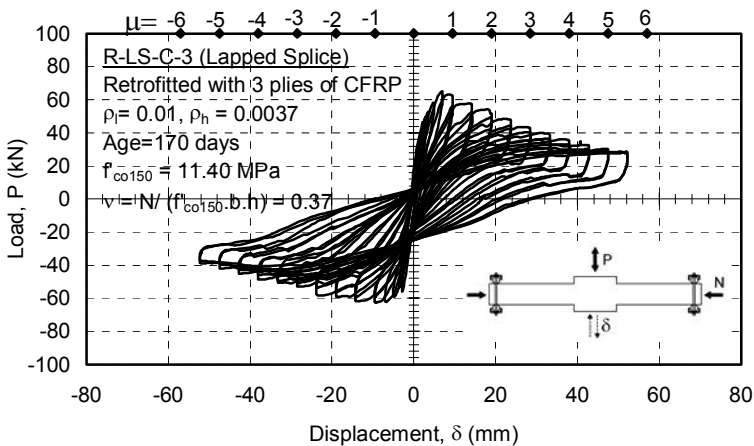


Fig. 10. Load-Displacement relationship and the appearance of the specimen R-LS-C-3

Specimen R-LS-C-6

Specimen R-LS-C-6 was retrofitted by 6 plies of CFRP sheets. The lateral load versus lateral displacement relationship measured at the stub is shown in Fig. 11. First bending cracks while pushing and pulling were observed around the stub faces at +2.39 mm and -2.34 mm displacements, respectively. Maximum load of +74 kN was reached at pushing cycle of the +7.0 mm displacement level. Crack widths were close to each other until the displacement ductility of $\mu=+1.0$ (+9.5 mm). However, crack widths increased significantly on the upper column afterwards. Damage increased at the displacement ductility of $\mu=\pm 4.0$ (± 38.0 mm) and crack widths changed between 0.3-0.5 mm at the lower column while they changed between 13-16 mm at the upper column. Test was stopped after completing the displacement ductility of $\mu=\pm 5.5$ (± 52.25 mm). R-LS-C-6 specimen at the end of the test is shown in Fig. 11.

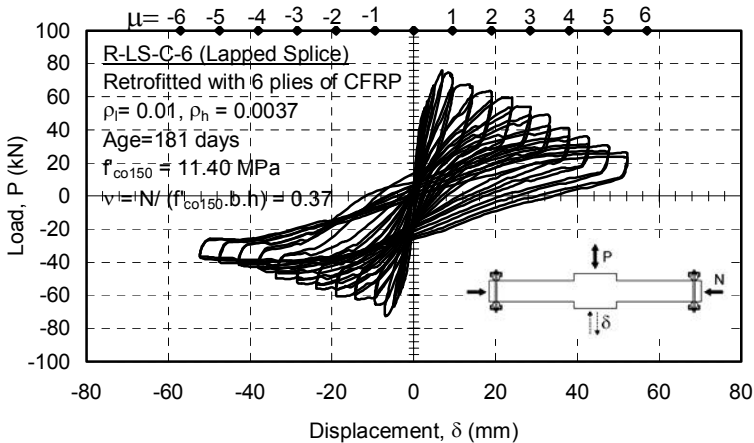


Fig. 11. Load-Displacement relationship and the appearance of the specimen R-LS-C-6

Specimen R-R-LS-C-6

Specimen R-LS-C-6 was repaired and then retrofitted by 6 plies of CFRP sheets. The lateral load versus lateral displacement relationship measured at the stub is shown in Fig. 12. First flexural cracks on the lower column while pushing and pulling were observed around the stub faces before the target displacement level of ± 2.8 mm. After displacement level of +7.0 mm first flexural crack on the upper column was observed. At the first displacement ductility of $\mu=+1.0$ (+9.5 mm), maximum lateral load was reached

(+72 kN) and light concrete crushing was observed on the lower column. R-R-LS-C-6 specimen at the end of the test is shown in Figure 12. Surprisingly, this specimen showed a better performance than R-LS-C-6 in terms of ductility.

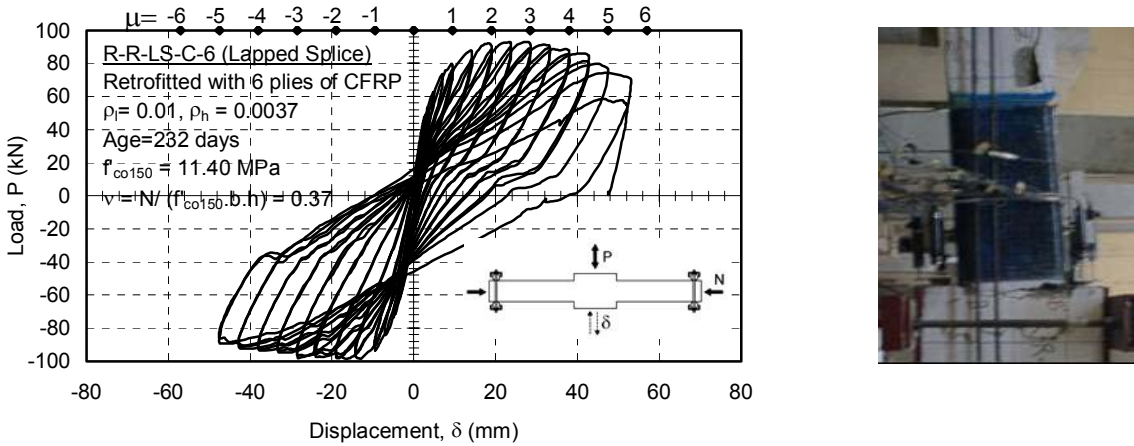


Fig. 12. Load-Displacement relationship and the appearance of the specimen R-R-LS-C-6

DISCUSSIONS

Comparisons of the envelope curves of lateral load-displacement relationships of the specimens with continuous and lapped splice longitudinal bars are given in Fig. 13 and 14, respectively.

The reference specimen with continuous longitudinal reinforcement, C-O-1, exhibited premature failure due to buckling of the longitudinal bars, while loss of bond caused premature failure for the reference specimen, LS-O-1, with inadequate lap splice length.

Retrofitted specimens R-C-C-3, R-C-C-6 and R-R-C-C-6 behaved similarly and exhibited an improved behavior in terms of ductility and strength. This showed that for the specimens with adequate lap splices, 3 plies of CFRP sheets provided similar enhancement as 6 plies of CFRP sheets, Fig. 13. For the specimen retrofitted with 3 plies of CFRP sheets, the strength increase was 25%, while it was 19% for the specimen retrofitted with 6 plies of CFRP sheets, and 37% for the specimen repaired and retrofitted with 6 plies of CFRP sheets. Note that these strength enhancement values are for pushing cycles.

As it can be seen from Fig. 13, reference specimen C-O-1 lost its strength significantly at the displacement ductility level of $\mu=+2.0$ (+19.0 mm), while retrofitted specimens R-C-C-3, R-C-C-6 and R-R-C-C-6, were still resisting 94%, 90% and 95% of their capacities at the displacement ductility level of $\mu=+4.0$ (+38.0 mm), respectively. Note that these values are for the first pushing cycle at the displacement ductility level of $\mu=+4.0$.

Lap spliced specimens had more remarkable strength degradations because loss of bond occurred even with a very small amount of transverse strain of concrete. Although an increase in the strength was observed for the retrofitted specimens, that strength could not be sustained throughout the loading. For the specimen retrofitted with 3 plies of CFRP sheets, strength increase was 19%, while it was 38% for the specimen retrofitted 6 plies of CFRP sheets, and 34% for the specimen repaired and retrofitted with 6 plies of CFRP sheets. Note that these strength enhancement values are for pushing cycles.

As it can be seen from Fig. 14, the reference specimen LS-O-1 lost its strength significantly after the displacement ductility level of $\mu=+1.0$ (+9.5 mm), while retrofitted specimens R-LS-C-3, R-LS-C-6 and

R-R-LS-C-6, were still resisting 54%, 53% and 82% of their capacities at the displacement ductility level of $\mu=+4.0$ (+38 mm), respectively.

It was observed that the flexural rigidities of the rc members were not significantly affected from the retrofitting. Consequently, only minor changes may be expected in the dynamic characteristics of the structure retrofitted with this technique.

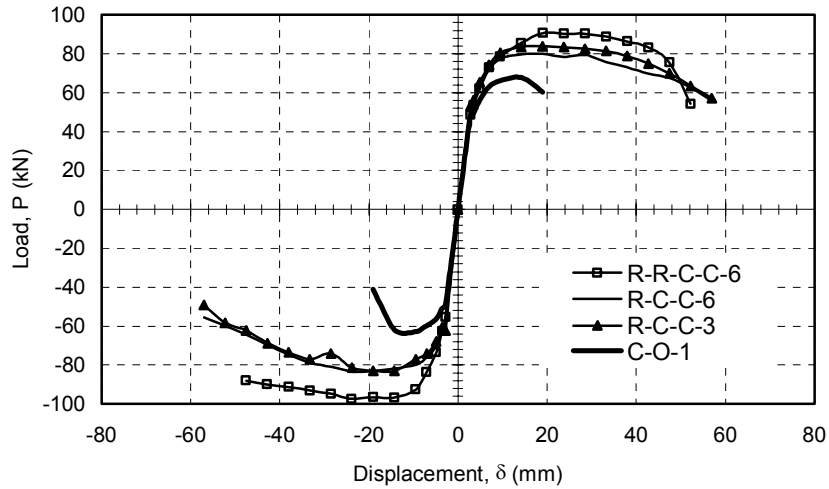


Fig. 13. Envelope lateral load-displacement relationships of the specimens with continuous longitudinal bars

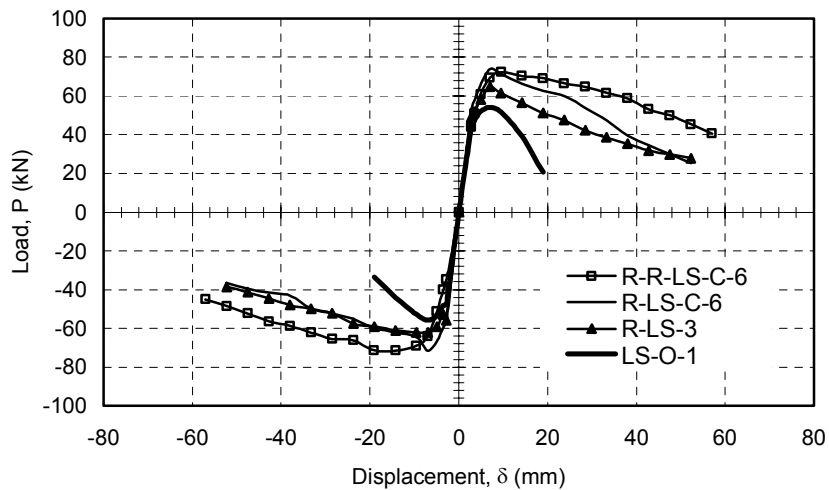


Fig. 14. Envelope lateral load-displacement relationships of the specimens with lap spliced longitudinal bars

CONCLUSIONS

At the end of the experimental work on the retrofit of plastic hinge regions of brittle reinforced concrete members under the combined action of axial load and reversed cyclic flexure, following conclusions are derived;

CFRP jackets improved the behavior of all specimens significantly both in terms of strength and ductility.

For specimens with continuous longitudinal reinforcement, CFRP jackets prevented premature strength loss by providing sufficient confinement that helped to prevent buckling of the longitudinal bars.

For specimens with lap spliced longitudinal reinforcement, CFRP jackets limited transverse deformations, that caused significant loss in strength due to reinforcement slip in the early stages of inelastic part of the loading for the original specimen.

For both cases (either continuous or lap spliced longitudinal reinforcement) thickness of the CFRP jacket had marginal effect on the behavior. Consequently it can be concluded that CFRP jackets of three plies were enough for the retrofit of these specimens.

Pre-damage of the specimens, did not have a significant adverse effect on the performance of the retrofitted specimens.

It should be noted that these conclusions are derived from a limited number of test results. For more general conclusions number of tests should be increased.

ACKNOWLEDGMENTS

The experimental work is financially supported by the The Scientific and Technical Research Council of Turkey (TUBITAK) and Yapkim Construction Chemicals Company. The contributions of Mr. C. Demir and Mr. E. Yilmaz during experimental work are also acknowledged.

REFERENCES

1. Kent DC, Park R. "Flexural members with confined concrete." ASCE Journal of the Structural Division 1971; 97(ST7): 1969-1990.
2. Mander JB, Priestley MJN, Park R. "Theoretical stress-strain model for confined concrete." ASCE Journal of the Structural Division 1988; 114(8): 1804-1826.
3. Mander, JB, Priestley MJN, Park R. "Observed stress-strain behavior of confined concrete." ASCE Journal of the Structural Division 1998; 114(8): 1827-1849.
4. Saatcioglu M, Ravzi SR. "Strength and ductility of confined concrete." ASCE Journal of the Structural Division 1992; 118(6): 1590-1607.
5. Ilki A, Ozdemir P, Fukuta T. "Confinement effect of reinforced concrete columns with circular cross-section". BRI Research Paper 1997; No. 143, Building Research Institute, Tsukuba, Japan.
6. Ilki A, Kumbasar N. "Compressive behavior of carbon fibre composite jacketed concrete with circular and non-circular cross sections." Journal of Earthquake Engineering 2003; 7(3): 381-406.
7. Ilki A, Kumbasar N. "Compressive behaviour of concrete strengthened by carbon fiber composite sheets." Structural Engineering and Mechanics 2002; 13(1): 75-90.
8. Ilki A, Kumbasar N, Koc V. "Low strength concrete members externally confined with FRP sheets" Structural Engineering and Mechanics; (accepted for publication).
9. Rochette P, Labossiere P. "Axial testing of rectangular column models confined with composites." Journal of Composites for Construction 2000; 4(3): 129-136.
10. Mirmiran A, Shahawy M. "Behaviour of concrete columns confined by fiber composites." ASCE Journal of Structural Engineering 1997; 123(5): 583-590.

11. Toutanji HA. "Stress-strain characteristics of concrete columns externally confined with advanced fiber composite sheets." *ACI Materials Journal* 1999; 96(3): 397-403.
12. Xiao Y, Wu H. "Compressive behaviour of concrete confined by carbon fiber composite jackets." *Journal of Materials in Civil Engineering* 2000; 12(2): 139-146.
13. Wang YC, Restrepo J. "Investigation of concentrically loaded reinforced concrete columns confined with glass fiber-reinforced polymer jackets." *ACI Structural Journal* 2001; 98(3): 377-385.
14. Lam L, Teng JG. "Design-oriented stress-strain model for FRP-confined concrete." *Construction and Building Materials* 2003; 17: 471-489.
15. Saadatmanesh H, Elsani MR, Jin L. "Repair of earthquake-damaged rc columns with FRP wraps." *ACI Structural Journal* 1997; 94(2): 206-215.
16. Seible F, Priestley MJN, Hegemier GA, Innamorato D. "Seismic retrofit of rc columns with continuous carbon fiber jackets." *Journal of Composites for Construction* 1997; 1(2): 52-62.
17. Ye L.P, Zhang K, Zhao SH, Feng P. "Experimental study on seismic strengthening of rc columns with wrapped CFRP sheets." *Construction and Building Materials* 2003; 17: 499-506.
18. Xiao Y, Ma R. "Seismic retrofit of rc circular columns using prefabricated composite jacketing." *Journal of Structural Engineering* 1997; 123(10): 1357-1364.
19. Rodriguez M, Park R. "Seismic load tests on reinforced concrete columns strengthened by jacketing." *ACI Structural Journal* 1994; 91(2): 150-159.
20. Wu YF, Griffith MC, Oehlers DJ. "Improving the strength and ductility of rectangular reinforced concrete columns through composites partial interaction: Test." *Journal of Structural Engineering* 2003; 129(9): 1183-1190.
21. Paulay, T. "Lapped splices in earthquake-resisting columns." *ACI Journal* 1982; 79: 458-469.
22. "Requirements for design and construction of rc structures (TS500-2000)." Turkish Standards Institute, Ankara, 2000.
23. Park R. "Evaluation of ductility of structures and structural assemblages from laboratory testing." *Bulletin of the New Zealand National Society for Earthquake Engineering* 1989; 22(3): 155-166.
24. Priestley MJN, Park R. "Strength and ductility of concrete bridge columns under seismic loading." *ACI Structural Journal* 1987; 84(1): 61-76.